

Embodied Geometric Intelligence (EGi) for Contact in Robots

Seyed Amir Tafrishi¹

¹Geometric Mechanics and Mechatronics in Robotics (gm²R) Lab, Engineering School, Cardiff, Wales, UK

E-mail: TafrishiSA@cardiff.ac.uk

Abstract. We introduce *embodied geometric intelligence* (EGi), a paradigm in which a robot’s morphology and passive compliance become active participants in perception, control, and manipulation. Leveraging underactuated or deformable bodies, soft robots exploit geometric cues in contact and environmental compliance to achieve traversal, grasping, and shape morphing without relying solely on onboard sensing or complex controllers. The term “geometry” traces to the Latin *geōmetría*, “gē” (land) + “metría” (measurement), highlighting knowledge acquired through contact. We formalize this approach using a curvature–compliance model unified with Montana’s contact kinematics, and we analyse the “dead fish in a stream” exemplar as a canonical case of geometry-driven control. Conceptual and mathematical results indicate that geometry-driven behaviors yield robustness and adaptability in dynamic, unstructured environments. This work lays the groundwork for a reimagined embodied intelligence that integrates geometry, physics, and control into a cohesive adaptive body.

1 Introduction

Robots are built to interact with their environment, yet they rarely exploit one of their greatest assets—passive physics. Traditional rigid designs dominate because they simplify control and guarantee predictable behavior. The rise of soft, compliant robots, however, offers a new opportunity: these bodies can leverage environmental forces to their advantage. At the same time, they expose the limits of conventional, fully actuated control schemes, which may be neither practical nor sufficient [2, 3, 4]. From a kinematic standpoint, the contact is intrinsically underactuated: even though, in principle, one can command up to three relative rotational rates and two tangential sliding velocities, the configuration evolves in five states, while practical platforms typically provide no more than three independent control inputs in various combinations specially in path planning scenarios [3].

From a current AI perspective, the robot’s body is more of a passive shell; it embodies knowledge and contributes directly to intelligent behavior [5]. Pfeifer and Bongard demonstrate that morphological computation allows mechanical structures to offload parts of their control computation into their physical form. However, modern AI-driven, physics-based learning methods—such as deep reinforcement learning for dexterous manipulation [6] and physics-simulation imitation [7]—often require massive datasets, struggle to generalize to novel (or takes heavy computation time), unstructured environments, and depend on centralized computation rather than leveraging embodied intelligence to support system operation. Ghost circuits, as introduced by Nanayakkara [8], leverage material compliance to form self-organizing feedback loops that yield robust, disturbance-driven behaviors from minimal inputs without data-intensive training. In mainstream robotics, however, contact has historically been modeled either as an exogenous disturbance to be rejected or as a hard constraint to be enforced by the controller

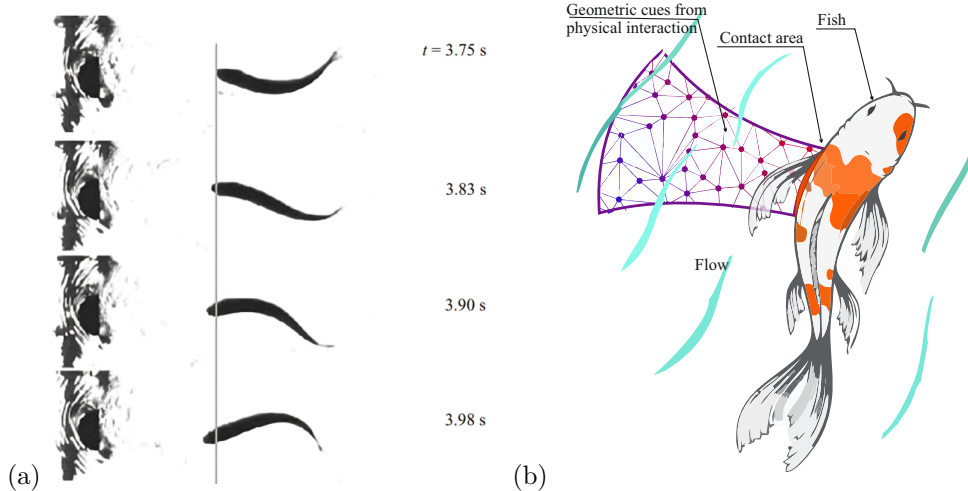


Figure 1: a) The dead fish in the stream experiment [1], b) The concept of Embodied Geometric Intelligence (EGi).

[9, 10]. In this problem, contact can play an important role. For example, more recent approaches explicitly treat contact as a resource: environment-exploiting manipulation and pushing mechanics formalize contact to achieve objectives [11], while contact-implicit trajectory optimization plans both motion and the sequence/timing of contacts within a single optimal-control problem [12, 13]. However, these methods typically assume extensive model knowledge and centralized control with rich sensing in order to accomplish narrowly specified tasks.

Some classical work in underactuated robotics [2, 3] and the concept of ghost circuits [8] reveal that compliant systems can give rise to rich, disturbance-driven or physics-based behaviours through minimal input (*underactuated*). These behaviors emerge not from explicit control, but from the smooth propagation of signals across dynamic system boundaries, enabled by material softness and exploited surrounding physics, which allows transient, self-organizing patterns of interaction to form, dissolve, and reconfigure spontaneously. Unlike rigid systems that require precise, centralized control, ghost circuits embody a kind of mechanical intelligence, where the morphology, environment, and observer all co-evolve as part of a dynamic feedback loop that defies replication but enables adaptive and robust behavior.

Biological systems, like bird wings [14], human passive walking [15], or fish bodies [16], achieve complex behaviors with remarkably few actuators by relying on morphology and compliance. Their joints and tissues passively adapt to external loads, creating rich, nonlinear dynamics that simplify rather than complicate control. One of the notorious and shocking examples was the dead fish in stream experiment from MIT [1] as shown in Fig. 1-a, where a fish body can stabilise and swim against the stream despite being dead. Inspired by these examples with particular focus on "dead fish scenario", we will propose "geometric intelligence" as a new control paradigm: by embedding intelligence directly into a robot's shape and deformability, we can build highly compliant, minimally actuated systems that remain robust in unstructured environments in contact. In this framework, the robot's geometry and passive mechanical properties serve as core elements of its control strategy. Localized mechanical interactions, rather than continuous global monitoring, enable robust locomotion over uneven terrain and dexterous manipulation with minimal sensing and actuation, exemplifying true geometric intelligence.

In more robotic and control examples rolling-sliding locomotion [3, 17], the contact point fundamentally characterises how a robot's surface engages with an environment or object. This engagement is governed by geometric properties such as normal curvature and geodesic torsion [3, 18], which dictate how relative angular motions at the kinematic level translate into movement between the robot and the surface. But when the contacting body, whether the robot's finger or the object, is soft, non-planar, and capable of complex, unpredictable deformations, an initially singular contact point can evolve into a compliance-dependent contact patch. How, then, can the robot continue to accomplish its task? Might we deliberately shape or locally control these deformations—modulating patch geometry—to boost manipulation dexterity, enhance locomotion, or even unlock novel physics-driven behaviors? Furthermore, how do locality and the distance from the actuator to the contact surface influence the governing geom-

Table 1: Positioning of EGi relative to Embodied Intelligence (EI), Morphological Computation (MC), and Physical Intelligence (PI).

Aspect	EI	MC	PI	EGi (this work)
Scope/goal	Body–environment–control coupling for intelligent behavior [5, 19, 20].	Quantify how morphology/environment contribute to behavior (body as computation) [21, 22].	Material/structural physics encode behaviors; minimal electronics common [23, 24].	Contact-centric geometric instantiation of EI: geometry and compliance as control variables during continuous contact.
Primary lens	Systems/behavior; architectural principles.	Information/measure of morphological contribution.	Materials, fields, stimuli-responsive mechanisms.	Differential geometry of contact; curvature/compliance co-design.
Mathematical anchor	Varies (control/behavior frameworks).	Information decomposition of sensorimotor loop; metrics.	Constitutive/material models; field–matter coupling.	Local kinematics; curvature tensors $\mathbf{K}(s)$, metrics $\mathbf{M}(s)$; compliance-weighted curvatures [18, 25, 17].
Parametrization	Typically time t .	Typically time t .	Often quasi-static or field-driven time scales.	Both time t and arclength s (contact-first); inputs/states can swap roles across patches.
Where it shines	General embodied control/learning settings.	Reasoning about how much the body of floods control.	Micro/meso-scale robots; passive/materially intelligent devices.	Contact-rich manipulation/locomotion; multi-contact planning (Darboux frame); unifying dynamic–structure (fluidic, soft or particle-based) and solid contact via curvature-driven local laws.

etry? Which additional physical parameters must be incorporated, and to what degree must a global control strategy detect and adapt to each local change? Finally, can we achieve this adaptability through **dependent underactuation**, where local **geometric mechanics** leverage a single primary actuator, or is a fully passive or semi-active strategy required? We will address some of these questions while also highlighting directions that could unlock new capabilities in robotics. Here, we propose *geometry* as a first-class variable—both in actuation space and configuration space—motivating semi- or fully independent, locally embodied control strategies.

The next big question is **Can we formulate a unified contact model, drawing inspiration from a fish’s body geometry interacting with flowing water, that leverages geometric descriptors to fuse environmental physics with a robot’s local dynamics, thus defining a new paradigm of Embodied Geometric Intelligence in Contact (EGi)?, as subset of embodied intelligence.** By embedding these geometric constraints into the control architecture, we can preserve essential locomotion capabilities (such as undulatory “swinging” motions in fish or snakes) while allowing the central controller to operate at a higher level of abstraction. In this framework, **geometric intelligence** serves as an intermediary layer that offloads low-level efficiency concerns, enabling the main controller to focus squarely on task objectives and goal achievement..

We situate **Embodied Geometric Intelligence (EGi)** within three established lines (Table 1). Embodied Intelligence (EI) treats intelligent behaviour as arising from the tight coupling of body, environment, and control—ranging from behaviour-based robotics to modern embodied AI [5, 19, 20]. Morphological Computation (MC) asks how much the body and environment “compute” for the controller, and provides formal, information-theoretic measures of the body’s contribution within the sensorimo-

tor loop [21, 22]. Physical Intelligence (PI) emphasises material/structural mechanisms that encode behaviours directly in physics (e.g., stimuli-responsive and field-driven devices), often with minimal on-board electronics, especially at micro/meso scales [23, 24].

$\mathcal{E}\mathcal{G}i$ is a contact-centric, geometric instantiation of EI for manipulation and locomotion under continuous contact, drawing on PI to realise adaptable bodies. $\mathcal{E}\mathcal{G}i$ elevates contact geometry to a first-class design and control variable and provides explicit differential-geometric operators that map patch-level state to force redistribution, torque generation, and orientation updates through transformed local contact kinodynamics [18]. Parameterising control in the arclength domain—rather than in time—reveals a contact-first structure in which quantities can swap roles across patches (what functions as an input at one patch may serve as a state at another), and it interfaces naturally with multi-contact planning in Darboux frames [25, 17], thereby decoupling sequencing from time. Relative to MC, $\mathcal{E}\mathcal{G}i$ replaces abstract information measures with local, control-usable geometric laws; relative to PI, it complements material transduction by prescribing contact-level geometry-to-actuation mappings at meso/macro scales, unifying interactions across soft, fluidic, granular, and solid media within a single geometric-mechanics view (see Table 1) which will conceptualize it through the dead fish experiment scenario.

2 Contact Geometry

2.1 Rolling Contact Background

Before exploring contact in the context of geometric intelligence ($\mathcal{E}\mathcal{G}i$), we briefly review the history of rolling contact and its use in robotics and control—summarising points developed in our recent technical survey [3]—and highlight their connection to $\mathcal{E}\mathcal{G}i$.

Across classical rolling-contact studies, several themes recur. First, *curvature-based local models* provide a common language: by expressing contact kinematics in the Gauss frame with shape operators, diverse systems reduce to first-order relations between surface curvatures and relative twist/slide. This viewpoint underlies controllability proofs for canonical pairs such as plate-ball and sphere-sphere, where curvature mismatch and nonholonomic brackets render the system bracket-generating and hence manoeuvrable [26]. Second, explicit geometric parametrisations enable constructive planning and analysis: alternative formulations streamline admissible rolling sets and constraints [27], while constructive motion generators and gait design yield practical trajectories for rolling systems [28]. Third, *contact as a control resource* supports manipulation strategies that exploit rather than avoid contact, with feedback structures and stability analyses clarifying how curvature and nonholonomy shape feasible behaviours [29]. Finally, higher-order extensions (for example, second-order models for ellipsoids) link local curvature to accelerations and inertial effects, improving trajectory tracking and model fidelity on complex surfaces [30]—an important consideration for integrating $\mathcal{E}\mathcal{G}i$. However, second-order contact geometry introduces strong dependencies on higher-order surface terms and Christoffel symbols, making computation and identification challenging [3]. In practice, first-order formulations such as Montana’s curvature-based contact model offer simpler state integration and are more readily incorporated into planning and control; accordingly, we focus on these models in what follows.

Taken together, these results motivate a pipeline that is now common in contact-rich robotics (assuming continuous contact): (i) adopt a curvature-centric local model to encode rolling-sliding constraints; (ii) use controllability structure to pick manoeuvre primitives (plate-ball, sphere-sphere) [26]; (iii) deploy simplified rolling maps or alternative formulations to prune admissible motions [27]; (iv) synthesise gaits or paths via constructive planners [28]; and (v) wrap the plan with feedback informed by contact-aware control analyses [29]. Recent surveys contextualise these ingredients for manipulation and locomotion, and highlight their utility when extended to compliant or reconfigurable platforms [17, 3].

Singular contact in a physically rotating system can be exemplified by a disk (car wheel) or a sphere (spherical robot) that obeys nonholonomic constraints and is driven by two rotational rates plus a spin; under a no-slip assumption, this model can be mapped to a cart-type planning system [31, 26]. For pure rolling spheres, motion planning splits into feedforward and feedback families: optimal-control approaches characterise extremals and elastica-like solutions for steering to a target configuration, while geometric-phase and Lie-bracket methods generate manoeuvre primitives for convergence [32, 33, 26, 28]. To handle contact-area limits and general convex shapes, polygonal or geodesic constructions and smooth C^∞ paths have been proposed, as well as numerical continuation for open-loop plans [34, 35, 28, 36]. Spin rolling introduces coupling via the spin angle; indirect spin strategies and feedback steering exist but can face controllability and conditioning issues under time scaling and frame changes [37, 38]. Recent Darboux-frame and arclength-based formulations compute curvature-guided, admissible trajectories and tunable convergence profiles without time parametrisation, though real-time closed-loop extensions on complex surfaces remain open [25, 17]. Open challenges include generalising to arbitrary geometries with online controllability checks and accommodating slippage, which perturbs the kinematics and can induce

drift—motivating planners that integrate robustness to slip and model uncertainty [39]. These points underscore that path planning for rolling contact remains an open problem, fundamentally dependent on how geometry mediates interaction. The challenge deepens when environmental dynamics act as a *virtual geometry*; in such cases, planners must not only generate feasible trajectories but also furnish structure for local controllers—a coupling that warrants further investigation.

The same sensing principles extend naturally from fingertip grasping to rolling shells and wheels: distributed tactile skins on spherical or cylindrical modules can measure normal pressure and tangential shear to (i) estimate local patch geometry (surface normal and principal curvatures), (ii) detect incipient slip, and (iii) infer contact–frame motion for haptic state estimation [40, 41, 42]. In grasping, multiple fingertips form a contact graph around an object; analogously, a multi–module rolling robot forms a time–varying contact graph against the environment (e.g., floor or pipe wall), where each patch supplies curvature and compliance estimates that feed the geometric state evolution and local controllers. This enables the same geometry–based loop to close control for locomotion—adjusting rolling velocities and compliance in response to contact cues—just as grasp controllers adjust fingertip forces and poses. Practically, vision–based tactile skins provide high–resolution shear/normal maps for patch estimation and slip detection [43, 42], while impedance layers regulate impact and maintain desired contact conditions [10]; together they allow unified planners to switch between grasp–like stabilisation (multi–patch bracing in clutter) and locomotion–like progression (sequential patching along a path) under a single curvature–compliance model [44].

2.2 The Paradigm of EGi from Dead Fish Scenario

We begin by introducing foundational definitions and perspectives on contact from a nontraditional standpoint, using illustrative examples to highlight the critical role of geometry—not only in classical rolling–contact mechanics but also in naturally occurring systems when contact is already exists (so not looking for discrete phases at this stage when contact may not exists).

A compelling example is MIT’s *dead fish in a stream* demonstration [1], shown in Fig. 1-b, which vividly illustrates how body geometry alone can give rise to an implicit control law. In this experiment, a rigid, fish-shaped object placed in a flowing stream naturally aligns itself tail-first into the current and maintains a stable orientation—entirely without sensing, actuation, or external control. This seemingly passive behavior can be understood through the lens of contact kinematics and fluid–structure interaction, revealing a form of geometric intelligence embedded in the object’s shape and compliance. In this paper, we explore the philosophy of this paradigm through example scenarios with connections to robotics.

To analyse the “dead fish” scenario, let \mathbf{u}_∞ be the uniform oncoming flow. Parameterise the wetted surface $\partial\Omega$ by arc length s with unit tangent $\hat{\mathbf{t}}(s)$ and unit normal $\hat{\mathbf{n}}(s)$. The local projections of the inflow are

$$\begin{aligned} u_n(s) &= \mathbf{u}_\infty \cdot \hat{\mathbf{n}}(s), \\ u_t(s) &= \mathbf{u}_\infty \cdot \hat{\mathbf{t}}(s). \end{aligned} \quad (1)$$

For gently curved surfaces, a leading–order representation of the near–surface velocity perturbed by curvature $\kappa(s)$ is

$$\mathbf{u}(s) \approx \mathbf{u}_\infty + \kappa(s) (\hat{\mathbf{n}}(s) \times \mathbf{u}_\infty),$$

which captures how curvature biases the local streamline turning and, through Bernoulli, the surface pressure. In viscous flow, the no–slip boundary layer generates vorticity $\boldsymbol{\omega} = \nabla \times \mathbf{u}$ from the wall–normal gradients of the tangential velocity; curvature modifies these gradients and hence the wall vorticity flux and shear stresses that contribute to the net torque [45, 46].

This perturbation captures the acceleration (or deceleration) of fluid around regions of convex curvature. By Bernoulli’s principle, the pressure on the surface is

$$p(s) \approx p_\infty + \frac{1}{2}\rho(\|\mathbf{u}_\infty\|^2 - \|\mathbf{u}(s)\|^2). \quad (2)$$

Integrating over all contact surface yields the net hydrodynamic force \mathbf{F} and moment $\boldsymbol{\tau}$ about the center of mass [47]:

$$\mathbf{F} = \int_{\partial\Omega} -p(s) \hat{\mathbf{n}}(s) \, dA, \quad (3)$$

$$\boldsymbol{\tau}(\theta) = \int_{\partial\Omega} (\mathbf{r}(s) \times [-p(s) \hat{\mathbf{n}}(s)]) \, dA, \quad (4)$$

where θ is the fish’s orientation relative to the flow. The curvature-induced pressure asymmetry produces a tail-first restoring torque that can be locally approximated by a linear stiffness law:

$$\tau_{\text{rest}}(\theta) \approx -K(\theta - \theta_0), \quad (5)$$

where θ_0 is the equilibrium alignment (typically π radians, tail-first) and K depends on the curvature distribution $\kappa(s)$. This expresses a *geometric control law* that can map orientation error directly to restoring moment via body shape that will be showcased next section.

The kinematic velocity gradient at each surface point decomposes into rolling (normal curvature) and sliding (tangential shear) contributions:

$$\nabla \mathbf{u}(s) = (\hat{\mathbf{t}} \otimes \hat{\mathbf{n}}) \kappa(s) \|\mathbf{u}_\infty\| + (\hat{\mathbf{t}} \otimes \hat{\mathbf{t}}) \partial_s u_t(s).$$

The first term generates centripetal pressure differences driving the restoring torque, while the second governs shear stress:

$$\tau(s) \approx \mu \partial_s u_t(s),$$

where μ is the fluid viscosity. By designing $\kappa(s)$ and a compliance profile $E(s)$ along the body, one prescribes the full fluid–structure feedback map.

We now formulate the input velocities by combining differential-geometry of contact with a curvature–flow model to obtain a unified relation. Specifically, we merge the fluid-induced motion with Montana’s five–state rolling–contact kinematics [18] by treating the flow contributions as the relative inputs $\boldsymbol{\omega}_{\text{rel}}$ and \mathbf{V}_{rel} , and evolve the state

$$\mathbf{x} = \begin{bmatrix} \mathbf{U}_f \\ \mathbf{U}_s \\ \psi \end{bmatrix}, \quad \mathbf{U}_f, \mathbf{U}_s \in \mathbb{R}^2, \quad \psi \in \mathbb{R},$$

where \mathbf{U}_f and \mathbf{U}_s are the local “fish” and “stream” coordinates in the Gauss frame, and ψ is the contact–patch torsion. At each surface point s , the fluid model provides

$$u_n(s) = \mathbf{u}_\infty \cdot \hat{\mathbf{n}}(s), \quad u_t(s) = \mathbf{u}_\infty \cdot \hat{\mathbf{t}}(s), \quad \kappa(s) \|\mathbf{u}_\infty\| \rightsquigarrow \text{rolling–velocity perturbation.}$$

Accordingly, we identify Montana’s relative motion inputs as

$$\boldsymbol{\omega}_{\text{rel}} = \begin{bmatrix} -\kappa(s) \|\mathbf{u}_\infty\| \\ 0 \\ 0 \end{bmatrix}, \quad \mathbf{V}_{\text{rel}} = \begin{bmatrix} u_t(s) \\ u_n(s) \\ 0 \end{bmatrix}.$$

Substituting into Montana’s kinematic equations [18], we obtain a generalized 3D formulation from a surface–model perspective:

$$\begin{aligned} \dot{\mathbf{U}}_f &= \mathbf{M}_f^{-1} (\mathbf{K}_f + \tilde{\mathbf{K}}_s)^{-1} \left(\begin{bmatrix} -\kappa \|\mathbf{u}_\infty\| \\ 0 \end{bmatrix} - \tilde{\mathbf{K}}_s \begin{bmatrix} u_t \\ u_n \end{bmatrix} \right), \\ \dot{\mathbf{U}}_s &= \mathbf{M}_s^{-1} \mathbf{R}_\psi (\mathbf{K}_f + \tilde{\mathbf{K}}_s)^{-1} \left(\begin{bmatrix} -\kappa \|\mathbf{u}_\infty\| \\ 0 \end{bmatrix} + \mathbf{K}_f \begin{bmatrix} u_t \\ u_n \end{bmatrix} \right), \\ \dot{\psi} &= \mathbf{T}_f \mathbf{M}_f \dot{\mathbf{U}}_f + \mathbf{T}_s \mathbf{M}_s \dot{\mathbf{U}}_s, \quad v_z = 0. \end{aligned} \quad (6)$$

where the sign in the first component of $\boldsymbol{\omega}_{\text{rel}}$ is chosen so that positive curvature induces a restoring rotation toward tail-first alignment (any consistent sign convention is acceptable); $\mathbf{M}_{(\cdot)}$, $\mathbf{K}_{(\cdot)}$, $\tilde{\mathbf{K}}_{(\cdot)}$, and $\mathbf{T}_{(\cdot)}$ denote the local metric, curvature, compliance-weighted curvature, and torsion operators in the Gauss frame, and \mathbf{R}_ψ maps the stream frame into the fish frame via the patch twist ψ . This mapping treats the fluid as a virtual rolling/sliding partner, capturing how curvature-biased flow generates effective relative twists and slips compatible with Montana’s contact kinematics for analysis and control. The construction is intentionally hypothetical: the geometric characteristics of the fish body $\{\mathbf{M}_f, \mathbf{K}_f, \mathbf{T}_f\}$ and the fluid stream $\{\mathbf{M}_s, \mathbf{K}_s, \mathbf{T}_s\}$ are interpreted to reproduce rolling–sliding interactions on the fish surface. Consequently, the geometries must be specified to encode the potential kinematic interaction of rolling and sliding on the surface; this leads directly to our unified contact model and its three core geometric–kinematic mappings:

- **Curvature-Driven Rolling:** The term $\kappa(s) \|\mathbf{u}_\infty\|$ in the relative angular velocity input reproduces centripetal pressure differentials, giving rise to the restoring torque $\tau_{\text{rest}}(\theta)$.
- **Compliance-Weighted Sliding:** The compliance matrix which embedded the normal curvature $\tilde{\mathbf{K}}_s$ acting on the slip vector $\begin{bmatrix} u_t \\ u_n \end{bmatrix}$ captures tangential shear feedback, recovering the viscous shear-stress relation $\tau(s) \approx \mu \partial_s u_t(s)$.
- **Morphology–Control Correspondence:** By setting normal curvature equations:

$$\mathbf{K}_f = \kappa(s) \mathbf{I}, \quad \tilde{\mathbf{K}}_s = E(s) \kappa(s) \mathbf{I},$$

the Montaña rolling–contact equations reduce precisely to

$$\tau_{\text{rest}}(\theta) = f(\kappa(\theta), \|\mathbf{u}_\infty\|) \approx -K(\theta - \theta_0), \quad (7)$$

showing that both fluid–structure and solid–solid contacts obey the same local torque law defined by curvature and compliance.

The primary challenge lies in interpreting the curvature matrix \mathbf{K}_f and compliance matrix $\tilde{\mathbf{K}}_s$ —originally defined for rigid rolling-sliding contacts—in the context of fluid-mediated alignment. By modeling the river flow interaction as an effective hybrid contact patch on a rigid fish body, we demonstrate that the same geometric descriptors govern both fluid–structure and solid–solid contacts. This synthesis confirms that curvature-based flow alignment and classical rolling/sliding mechanics obey a single, geometry-driven kinematic law, unifying disparate contact phenomena under the banner of *geometric intelligence*.

To make this unification concrete, we approximate each infinitesimal patch of the fish’s body by its osculating sphere. Classic fluid mechanics shows that the pressure around a sphere in a flow is lower on the rear half than the front because of wake losses, and this pressure differential produces a net force and restoring moment; a simple demonstration is the stability of a table-tennis ball suspended in a jet[48]. By assigning a local curvature $\kappa(s)$ and thus a radius $R = 1/\kappa(s)$ to each patch, we can estimate the fluid-induced torque using sphere formulas and treat the fluid’s influence as a “virtual” rolling contact partner. Our hypothesis is that vortices shed along the fish body form concentric circular flows that mimic a compliant contact surface; their radii and strength depend on $u_t(s)$ and the viscosity μ , which is captured in the compliance term $\tilde{\mathbf{K}}_s$. Classical explanations of station-keeping and upstream motion behind cylinders (dead fish; Kármán gait) attribute behavior to resonance with the vortex street and pressure/shear asymmetries that can yield net thrust or reduced energetic cost [1, 49, ?] with using conventional rigid-body dynamic modeling (spring-damper-mass). Our treatment isolates the alignment/stability mechanism via curvature-induced restoring torques and maps it to contact kinematics by interpreting the flow as a virtual rolling partner. Passive propulsion in wakes requires unsteady coupling to the vortex street and energy extraction, which lies beyond the quasi-steady alignment model here. We therefore restrict claims in this section to orientation/stability; propulsion via unsteady vortex locking is discussed as future work.

Moreover, experimental soft robots demonstrate that geometric asymmetry alone can induce self-turning and navigation in complex mazes without a central controller [50]. This suggests that by tuning the curvature and compliance distribution along a robot’s body, we can encode a local control law that exploits environmental flow instead of fighting it. In engineered reconfigurable robots, our framework therefore predicts that modules with adjustable curvature will generate desired trajectories simply by changing shape; for biological organisms, it offers a geometric explanation for how fish harness body curvature and passive elasticity to maintain orientation or generate thrust which will be future work of our study.

3 Embodied Geometric Intelligence (EGi)

A soft-robotic analogue embeds a prescribed curvature–compliance distribution into its passive elasticity, yielding a morphology that computes alignment in a flowing medium through its material and form alone. This geometric intelligence layer autonomously handles stability and orientation, freeing a higher-level controller to focus exclusively on task planning.

MIT’s “dead fish” experiment exemplifies this concept: a rigid, fish-shaped body released in a uniform stream naturally aligns tail-first without any sensing or actuation. At the core of this passive alignment is the local curvature $\kappa(s)$, which perturbs fluid pressures via Bernoulli’s principle and curvature-induced accelerations, producing a net restoring torque $\tau_{\text{rest}}(\theta) = f(\kappa(\theta), \|\mathbf{u}_\infty\|)$ based on (7) where $\theta_0 = \pi$ represents the stable tail-first orientation. Here, the body’s geometry $\kappa(s)$ plays a dual role: it indirectly

senses flow direction through the pressure distribution $\Delta p(s)$ induced on the skin from (2), and it actuates reorientation via the resulting torque $\tau(s)$. This yields an important closed morpho-fluid feedback loop that lies EGi paradigm as

$$\kappa(s) \longrightarrow \Delta p(s) \longrightarrow \tau(s) \longrightarrow \theta_{\text{new}},$$

in which $\kappa(s)$ sets sensitivity, $\Delta p(s)$ is the sensed proxy of flow, $\tau(s)$ is the passive actuation, and θ_{new} is the updated orientation. This paradigm extends naturally to soft robots in fluids, granular media, or over deformable terrain. By shaping surface curvature and distributing compliance, one can replicate passive stabilization and alignment in reconfigurable, compliant bodies. In such systems, softness provides the substrate for embodied geometric intelligence: parts of sensing and control are offloaded to morphology [51, 52]. Practically, the same mechanics—expressed either as surface pressure integrals or as local curvature maps—translate into patchwise control laws embedded in the shell, reducing the burden on central controllers. To make the connection between pressure fields and the linear stiffness law $\tau_{\text{rest}}(\theta) \approx -K(\theta - \theta_0)$ precise without over-modeling, work at the per-area level rather than equating an integral to a pointwise term. We can also define the torque density from (4) as input about the control axis $\hat{\mathbf{e}}_\theta$,

$$t(s, \theta) := (\mathbf{r}(s) \times [-p(s, \theta) \hat{\mathbf{n}}(s)]) \cdot \hat{\mathbf{e}}_\theta,$$

then introduce the geometric stiffness density $k(s) := -\partial t / \partial \theta|_{\theta_0}$ and recover the global stiffness by integration, $K = \int_{\partial\Omega} k(s) dA$. This cleanly links local curvature-pressure effects to the global restoring torque.

Because each infinitesimal patch of the soft robot’s surface enacts the same curvature-driven feedback law independently, no centralized, low-level controller is needed to maintain stability. Instead, the robot’s morphology and material properties “compute” part of the control, simplifying the architecture and enabling fast, adaptive responses [51]. A supervisory controller therefore only issues high-level objectives—such as waypoints or manipulation goals—while the body’s geometry ensures robust passive adaptation to environmental uncertainties. This division of labor between body and controller embodies the core idea of morphological intelligence [52], where physical characteristics influence perception and cognitive processing.

By tuning curvature profiles, introducing stiffness gradients, or incorporating anisotropic compliance, designers can unlock a spectrum of passive behaviors: station keeping in currents, wave surfing, adaptive squeezing through constrictions, and more. Recent work on soft robotic rollers shows that geometric asymmetry and material intelligence can produce sustained self-turning and maze escaping without explicit control [50], demonstrating that shape itself can encode a control policy. These findings support the view that geometric intelligence is a first-class element of robot design: by manipulating curvature and compliance, complex behaviors are achievable with minimal sensing and actuation, bridging morphology, physics, and control in a unified, semi-autonomous system. From the robot’s perspective, underactuation provides a complementary pathway to tune compliance and curvature with minimal hardware, for example via local surface transformations driven by pneumatic inflation [53]—though potentially energy intensive due to pressurization—or by cable-driven skins that realize primarily pull-only deformations [54]. However, these mechanisms can be constrained—some demand substantial energy (e.g., pneumatics), others offer mainly one-direction actuation (e.g., cable skins). A key research direction is to maximise the use of environmental forces and reserve minimal, localized actuation for on-demand adjustments, keeping the primary structure and high-level controller lean, efficient, and focused on mission objectives.

The principles above align with morphological computation: in biological and soft robots, stiffness modulation and body deformation enable safe interaction with uncertainty while exploiting passive dynamics to simplify control [51]. Embodied intelligence emphasizes that information processing is distributed across body, sensors, actuators, and environment [55]. By embedding curvature and compliance profiles into the structure, the surface itself becomes an information-processing interface that interprets environmental forces and generates appropriate responses. In grasping, compliant fingertips combined with proximity sensing (optical, capacitive, electric field, time-of-flight) provide short-range ranging and approach direction before touch; when fused with tactile measurements they improve contact localization, slip prediction, and low-force acquisition [56]. Passive and underactuated fingertip designs exploit compliance to adapt shape with minimal control effort [57], yet integrating proximity and tactile sensing at fingertip scale remains challenging due to power, wiring, and calibration constraints, especially when the fingertip must also deform. This extends to soft mobile rolling on general terrains. Consider a soft spherical shell (nominal radius R) in continuous contact. In (6), replace the rigid-body curvature operator by the deformation-dependent convex-surface shell operator $\mathbf{K}_s^*(s)$ (with entries $1/R_{i,\text{eff}}(s)$) and the environment by its shape operator $\mathbf{K}_e(s)$ expressed in the contact frame. Compliance $E(s)$ enters via $R_{i,\text{eff}}(s) = R + \delta R_i(E(s), \text{load})$, thus co-designing geometry and compliance. In the locally isotropic

limit ($\mathbf{K}_s^* = \kappa_s \mathbf{I}$, $\mathbf{K}_e = \kappa_e \mathbf{I}$) one recovers the expected scalar composition $\kappa_{\text{eff}}(s) = \kappa_s(s) + \kappa_e(s)$ and the standard spherical rolling (no-slip) relation without reprinting formulas. Consequently, spatial patterns in $\kappa_s(s)$ and $E(s)$ around the contact ring modulate $\Delta F(s)$ and $\tau(s)$, enabling curvature-guided steering and stabilisation on general ground geometries with minimal sensing [3]. Within the EG*i* perspective, these fingertip/robot-surface contact signals act as local estimates of the curvature and compliance map, tuning patch-level behavior so that the global controller remains simple. This synergy between morphology and control improves energy efficiency and robustness and enables reconfigurable robots that adapt their form in real time.

4 Conclusion

We presented Embodied Geometric Intelligence (EG*i*) as a unifying view of contact in which geometry and compliance act as distributed sensing and actuation that convert environmental loads into stabilising actions while a light supervisory layer handles high level goals. Using the dead fish scenario as a guide, we derived a local geometric control law that explains tail first alignment and showed how the same principle maps to rolling compliant shells, soft mobile robots, and contact driven grasping or more complex robotics platforms.

In practice, EG*i* yields clear design rules: place geometric anisotropy where it matters, distribute compliance to set gains and damping, and use sparse pressure or shear cues to adapt locally with minimal actuation. This supports robust, low power grasping, locomotion, and reconfiguration in cluttered or hazardous settings. Open challenges include selecting the minimum actuation capable of meaningful shape or stiffness change, allocating surface properties across the body, and quantifying the contribution of embodied geometric intelligence to system performance. Future work will validate local to global effects of geometry in hardware and simulation, develop real time estimators from sparse contact signals, engineer variable shape and variable stiffness mechanisms, and extend EG*i* to unsteady flows, granular media, and deformable terrain with basic stability guarantees.

This work is conceptual and analytical to open a new view in the field of robotics through contact and geometric mechanics. It explores the philosophical view and how to bring the analytical framework into practice for control implementation. For future robotic application, we will: (i) run patchwise simulations coupling the stiffness density $k(s)$ with the five-state contact model in (6) with rolling contact robotic examples [3]; (ii) perform benchtop tests on a quasi-compliant-spherical rolling shell with reconfigurable curvature bands and tunable compliance on uneven terrains and understand feasibility of embodied contact intelligence concept; and (iii) test a rigid–soft body interaction with fluid similarities to fish scenario in a laminar jet to measure $\tau_{\text{rest}}(\theta)$ versus $\kappa(s)$ and $E(s)$. We will quantify robustness and energy, and compare against MC and PI baselines where shape is not treated as a first-class variable.

References

- [1] D. N. Beal, F. S. Hover, M. S. Triantafyllou, J. C. Liao, and G. V. Lauder, “Passive propulsion in vortex wakes,” *Journal of fluid mechanics*, vol. 549, pp. 385–402, 2006.
- [2] B. He, S. Wang, and Y. Liu, “Underactuated robotics: a review,” *Int. J. Adv. Rob. Syst.*, vol. 16, no. 4, p. 1729881419862164, 2019.
- [3] S. A. Tafriahi, M. Svinin, and K. Tahara, “A survey on path planning problem of rolling contacts: Approaches, applications and future challenges,” *arXiv preprint arXiv:2501.04442*, 2025.
- [4] D. Trivedi, C. D. Rahn, W. M. Kier, and I. D. Walker, “Soft robotics: Biological inspiration, state of the art, and future research,” *Applied bionics and biomechanics*, vol. 5, no. 3, pp. 99–117, 2008.
- [5] R. Pfeifer and J. Bongard, *How the Body Shapes the Way We Think: A New View of Intelligence*. Cambridge, MA: MIT Press, 2006.
- [6] M. Andrychowicz, B. Baker, M. Chociej, R. Józefowicz, B. McGrew, J. Pachocki, A. Petron, M. Plappert, G. Powell, A. Ray, J. Schneider, S. Sidor, J. Tobin, P. Welinder, L. Weng, and W. Zaremba, “Learning dexterous in-hand manipulation,” in *Proceedings of the IEEE International Conference on Robotics and Automation (ICRA)*, pp. 2248–2255, 2018.
- [7] X. B. Peng, G. Berseth, K. Gupta, and M. van de Panne, “Deepmimic: Example-guided deep reinforcement learning of physics-based character skills,” in *Proceedings of the ACM SIGGRAPH/Eurographics Symposium on Computer Animation*, pp. 1–14, 2018.
- [8] T. Nanayakkara, *Handbook on Soft Robotics*. Springer, 2024.

- [9] M. T. Mason, *Mechanics of Robotic Manipulation*. MIT Press, 2001.
- [10] N. Hogan, “Impedance control: An approach to manipulation—part i: Theory,” *Journal of Dynamic Systems, Measurement, and Control*, vol. 107, no. 1, pp. 1–7, 1985.
- [11] K. M. Lynch and M. T. Mason, “Stable pushing: Mechanics, controllability, and planning,” *The International Journal of Robotics Research*, vol. 15, no. 6, pp. 533–556, 1996.
- [12] M. Posa, C. Cantu, and R. Tedrake, “A direct method for trajectory optimization of rigid bodies through contact,” *The International Journal of Robotics Research*, vol. 33, no. 1, pp. 69–81, 2014.
- [13] I. Mordatch, E. Todorov, and Z. Popović, “Discovery of complex behaviors through contact-invariant optimization,” *ACM Transactions on Graphics*, vol. 31, no. 4, pp. 43:1–43:7, 2012.
- [14] K. A. Hoffmann, T. G. Chen, M. R. Cutkosky, and D. Lentink, “Bird-inspired robotics principles as a framework for developing smart aerospace materials,” *Journal of Composite Materials*, vol. 57, no. 4, pp. 679–710, 2023.
- [15] R. Tedrake, “Underactuated robotics: Learning, planning, and control for efficient and agile machines course notes for mit 6.832,” *Working draft edition*, vol. 3, no. 4, p. 2, 2009.
- [16] J. E. Colgate and K. M. Lynch, “Control problems solved by a fish’s body and brain: A review,” *Mechanical Engineering Department, Northwestern University*, 2004.
- [17] S. A. Tafrihi, M. Svinin, M. Yamamoto, and Y. Hirata, “A geometric motion planning for a spin-rolling sphere on a plane,” *Applied Mathematical Modelling*, vol. 121, pp. 542–561, 2023.
- [18] D. J. Montana, “The kinematics of contact and grasp,” *Int. J. Robot. Res.*, vol. 7, no. 3, pp. 17–32, 1988.
- [19] R. Pfeifer, M. Lungarella, and F. Iida, “Self-organization, embodiment, and biologically inspired robotics,” *Science*, vol. 318, no. 5853, pp. 1088–1093, 2007.
- [20] R. A. Brooks, “Intelligence without representation,” *Artificial Intelligence*, vol. 47, no. 1–3, pp. 139–159, 1991.
- [21] H. Hauser, A. J. Ijspeert, R. M. Fuchslin, R. Pfeifer, and W. Maass, “Towards a theoretical foundation for morphological computation with compliant bodies,” *Biological Cybernetics*, vol. 105, no. 5-6, pp. 355–370, 2012.
- [22] K. G. Zahedi and N. Ay, “Quantifying morphological computation,” *Entropy*, vol. 15, no. 5, pp. 1887–1915, 2013.
- [23] M. Sitti, “Physical intelligence as a new paradigm,” *Extreme Mechanics Letters*, vol. 46, p. 101340, 2021.
- [24] X. Fan, X. Dong, A. C. Karacakol, H. Xie, and M. Sitti, “Reconfigurable multifunctional ferrofluid droplet robots,” *Proceedings of the National Academy of Sciences*, vol. 117, no. 45, pp. 27916–27926, 2020.
- [25] S. A. Tafrihi, M. Svinin, and M. Yamamoto, “Darboux-frame-based parametrization for a spin-rolling sphere on a plane: A nonlinear transformation of underactuated system to fully-actuated model,” *Mech. Mach. Theory*, vol. 164, p. 104415, 2021.
- [26] Z. Li and J. Canny, “Motion of two rigid bodies with rolling constraint,” *IEEE Trans. Robot. Autom.*, vol. 6, no. 1, pp. 62–72, 1990.
- [27] A. Bicchi and A. Marigo, “Rolling contacts and dexterous manipulation,” in *Proc. IEEE In. Conf. Robot. Autom.*, vol. 1, pp. 282–287, IEEE, 2000.
- [28] M. Svinin and S. Hosoe, “Motion planning algorithms for a rolling sphere with limited contact area,” *IEEE Trans. Robot.*, vol. 24, no. 3, pp. 612–625, 2008.
- [29] K. M. Lynch and T. D. Murphey, “Control of nonprehensile manipulation,” in *Control problems in robotics*, pp. 39–57, Springer, 2003.

- [30] Z. Woodruff and K. Lynch, “Second-order contact kinematics between three-dimensional rigid bodies,” *Journal of Applied Mechanics*, vol. 86, no. 8, 2019.
- [31] J.-P. Laumond, *Robot motion planning and control*, vol. 229. Springer, 1998.
- [32] V. Jurdjevic, “The geometry of the plate-ball problem,” *Arch. Ratio. Mech. Anal.*, vol. 124, no. 4, pp. 305–328, 1993.
- [33] Y. Sachkov, “Maxwell strata and symmetries in the problem of optimal rolling of a sphere over a plane,” *Sb. Math.*, vol. 201, no. 7, pp. 1029–1051, 2010.
- [34] A. Bicchi and A. Marigo, “Dexterous grippers: Putting nonholonomy to work for fine manipulation,” *Int. J. Robot. Res.*, vol. 21, no. 5-6, pp. 427–442, 2002.
- [35] K. Harada, T. Kawashima, and M. Kaneko, “Rolling based manipulation under neighborhood equilibrium,” *Int. J. Robot. Res.*, vol. 21, no. 5-6, pp. 463–474, 2002.
- [36] F. Alouges, Y. Chitour, and R. Long, “A motion-planning algorithm for the rolling-body problem,” *IEEE Trans. Robot.*, vol. 5, no. 26, pp. 827–836, 2010.
- [37] H. Date, M. Sampei, M. Ishikawa, and M. Koga, “Simultaneous control of position and orientation for ball-plate manipulation problem based on time-state control form,” *IEEE Trans. Robot.*, vol. 20, no. 3, pp. 465–480, 2004.
- [38] G. Oriolo and M. Vendittelli, “A framework for the stabilization of general nonholonomic systems with an application to the plate-ball mechanism,” *IEEE Trans. Robot.*, vol. 21, pp. 162–175, April 2005.
- [39] A. Morinaga, M. Svinin, and M. Yamamoto, “A motion planning strategy for a spherical rolling robot driven by two internal rotors,” *IEEE Trans. Robot.*, vol. 30, no. 4, pp. 993–1002, 2014.
- [40] R. S. Dahiya, G. Metta, M. Valle, and G. Sandini, “Tactile sensing—from humans to humanoids,” *IEEE Transactions on Robotics*, vol. 26, no. 1, pp. 1–20, 2010.
- [41] N. F. Lepora, “Soft biomimetic optical tactile sensing with the tactip: A review,” *IEEE Sensors Journal*, vol. 21, no. 19, pp. 21131–21143, 2021.
- [42] S. Yuan, S. Wang, R. Patel, M. Tippur, C. Yako, E. Adelson, and K. Salisbury, “Tactile-reactive roller grasper,” *arXiv preprint arXiv:2306.09946*, 2023.
- [43] S. Dong, W. Yuan, and E. H. Adelson, “Improved gelsight tactile sensor for measuring geometry and slip,” in *Proceedings of the 2017 IEEE/RSJ International Conference on Intelligent Robots and Systems (IROS)*, pp. 137–144, IEEE, 2017.
- [44] N. F. Lepora and J. Lloyd, “Pose-based tactile servoing: Controlled soft touch using deep learning,” *IEEE Robotics & Automation Magazine*, vol. 28, no. 4, pp. 43–55, 2021.
- [45] H. Schlichting and K. Gersten, *Boundary-Layer Theory*. Berlin, Heidelberg: Springer, 9 ed., 2017.
- [46] G. K. Batchelor, *An Introduction to Fluid Dynamics*. Cambridge: Cambridge University Press, 1967.
- [47] T. Y. Wu, “Hydromechanics of swimming propulsion. part 1. swimming of a two-dimensional slender fish,” *Journal of Fluid Mechanics*, vol. 10, no. 2, pp. 321–344, 1961.
- [48] P. University, “Bernoulli’s equation and pressure distribution.” <https://www.princeton.edu/> Accessed 13 Aug. 2025.
- [49] J. C. Liao, D. N. Beal, G. V. Lauder, and M. S. Triantafyllou, “The kármán gait: novel body kinematics of rainbow trout swimming in a vortex street,” *Journal of Experimental Biology*, vol. 206, no. 6, pp. 1059–1073, 2003.
- [50] Y. Zhao, Y. Hong, Y. Li, *et al.*, “Physically intelligent autonomous soft robotic maze escaper,” *Science Advances*, vol. 9, no. eadi3254, pp. 1–9, 2023.
- [51] C. Laschi and M. Cianchetti, “Soft robotics: new perspectives for robot bodyware and control,” *Frontiers in Bioengineering and Biotechnology*, vol. 2, p. 3, 2014.

- [52] R. Pfeifer and J. Bongard, *How the Body Shapes the Way We Think: A New View of Intelligence*. MIT Press, 2007.
- [53] N. El-Atab, R. B. Mishra, F. Al-Modaf, L. Joharji, A. A. Alsharif, H. Alamoudi, M. Diaz, N. Qaiser, and M. M. Hussain, “Soft actuators for soft robotic applications: A review,” *Advanced Intelligent Systems*, vol. 2, no. 10, p. 2000128, 2020.
- [54] M. Krysov and S. A. Tafirishi, “Development of underactuated geometric compliant (ugc) module with variable radial for robotic applications,” in *Annual Conference Towards Autonomous Robotic Systems*, pp. 195–207, Springer, 2024.
- [55] Z. Zhao, Q. Wu, J. Wang, B. Zhang, C. Zhong, and A. A. Zhilenkov, “Exploring embodied intelligence in soft robotics: A review,” *Biomimetics*, vol. 9, no. 4, p. 248, 2024. Open access review on morphological and embodied intelligence.
- [56] S. E. Navarro, S. Mühlbacher-Karrer, H. Alagi, H. Zangl, K. Koyama, B. Hein, C. Duriez, and J. R. Smith, “Proximity perception in human-centered robotics: A survey on sensing systems and applications,” *IEEE Trans. Robot.*, vol. 38, no. 3, pp. 1599–1620, 2021.
- [57] R. Ozawa and K. Tahara, “Grasp and dexterous manipulation of multi-fingered robotic hands: a review from a control view point,” *Advanced Robotics*, vol. 31, no. 19-20, pp. 1030–1050, 2017.